ICSV13 - Vienna
The Thirteenth International Congress on Sound and Vibration
Vienna, Austria, July 2-6, 2006

A Volumetric Acoustic Intensity Probe based on Spherical Nearfield Acoustical Holography

Earl G. Williams

Naval Research Laboratory
4555 Overlook Ave
Washington DC, USA
williams@pa.nrl.navy.mil

Abstract
An unusual and unique marriage of high level mathematics and metrology has led to the design and construction of a device that measures instantaneously the vector acoustic intensity throughout a cubic volume. In this volume the device provides either the instantaneous time domain or the frequency domain intensity field. Called the Volumetric Acoustic Intensity Probe (VAIP) this device provides the ability to locate sources of sound in the interior spaces (or exterior) of ships, military vehicles, aircraft, etc, by mapping the magnitude and direction of the flow of acoustic intensity throughout the measurement volume in the frequency band from 0 to 1400 Hz. The probe consists of a nearly transparent spherical array of 50 microphones optimally positioned on an imaginary spherical surface and uses spherical NAH to convert the microphone pressures into a vector intensity field in a volume centered on the sphere origin. The array has a radius of 0.2m and the reconstruction volume is limited to a maximum radius of 0.4m. Front-end signal processing for the VAIP is designed to deal with random, non-stationary acoustic fields by creating partial field holograms, constructed using either SVD or Cholesky decomposition methods from ensemble averages of the cross-spectral densities with fixed references or with vertex array microphones. In a major application of this approach, experimental results taken during the flight of a Boeing 777 aircraft will be discussed. These results show excellent success at locating the dominant sound sources near the array.

INTRODUCTION

Spherical microphone arrays have a long history of use in acoustics and often the theory of operation of these systems, like the probe discussed here, is based in spherical harmonic

decompositions. Two early implementations were significant in acoustics[1, 2] and a very recent paper provides a good review.[3] However, almost all of this research has been aimed at a prediction of the far-field from near-field measurements, a forward problem that is mathematically well posed. In the research presented here no far-field assumption is made and the more difficult inverse problem is solved - prediction of the sound field between the array and the sources of sound. However, unlike the popular single axis and multiple axis vector intensity probes that provide high measurement accuracy at a single point, the VAIP provides the vector intensity at hundreds of points instantaneously, trading off high accuracy to image the intensity vector field throughout a sizable volume.

THEORY OF OPERATION

The spherical coordinate system is by far the ideal for the implementation of nearfield acoustical holography (NAH) as the finite aperture problem is nonexistent. A photograph of the 50 element spherical array is shown in fig. l. A spherical reconstruction volume $\mathcal{V}$, defined by

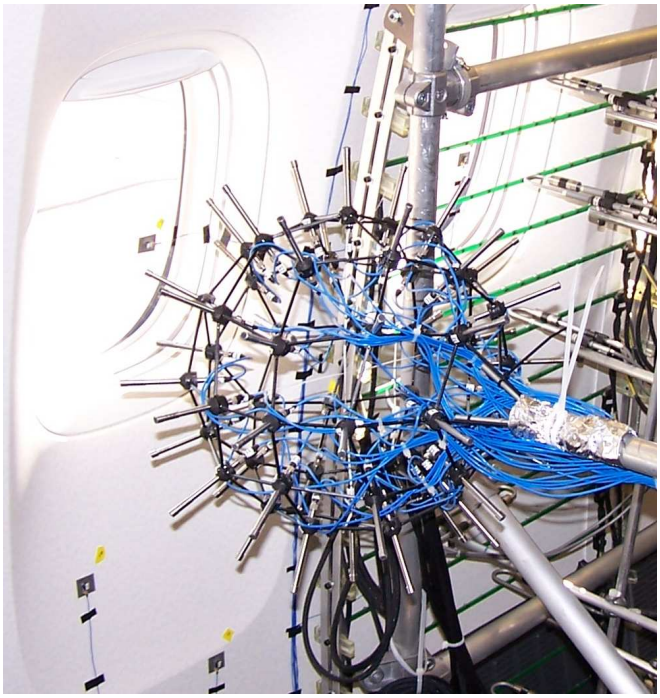

Figure 1: The NRL Spherical Array with 50 microphones set up for noise measurements inside a Boeing 777 aircraft

spherical coordinates $\mathbf{r} = (r, \theta, \phi) \in \mathcal{V}$ and of extent $0 \leq r \leq r_{max}$, is source free except for a "transparent" microphone array structure with sensors located at $r = a < r_{max}$. The

acoustic pressure $p_\infty(\mathbf{r},\omega)$ is approximated anywhere in $\mathcal{V}$ by a finite sum given by[4]

$$p_\infty(\mathbf{r},\omega) \approx p_N(\mathbf{r},\omega) \equiv \sum_{n=0}^{N} \frac{j_n(kr)}{j_n(ka)} \sum_{m=-n}^{n} P_{mn}(a,\omega) Y_n^m(\theta,\phi), \tag{1}$$

where $Y_n^m(\theta,\phi)$ are orthonormal spherical harmonics, j_n are spherical Bessel functions and $k=\omega/c$. This approximation becomes exact in the limit as $N\to\infty$. Measurements are made in the time domain and p_∞ is derived from a temporal Fourier transform of the measured pressure in the usual way. The unknowns P_{mn} in this equation are called the Fourier coefficients. The acoustic velocity vector is given in terms of the unknown Fourier coefficients[4]:

$$v_\theta(\mathbf{r},\omega) = \frac{1}{i\omega\rho} \sum_{n=0}^{N} \frac{j_n(kr)}{r j_n(ka)} \sum_{m=-n}^{n} P_{mn} \frac{\partial Y_n^m(\theta,\phi)}{\partial\theta} \tag{2}$$

$$v_\phi(\mathbf{r},\omega) = \frac{1}{i\omega\rho} \sum_{n=0}^{N} \frac{j_n(kr)}{r j_n(ka)} \sum_{m=-n}^{n} P_{mn} \frac{imY_n^m(\theta,\phi)}{\sin\theta} \tag{3}$$

$$v_R(\mathbf{r},\omega) = \frac{1}{i\rho c} \sum_{n=0}^{N} \frac{j_n'(kr)}{j_n(ka)} \sum_{m=-n}^{n} P_{mn} Y_n^m(\theta,\phi), \tag{4}$$

where the equalities hold strictly only in the limit as $N\to\infty$. The active intensity vector $\vec{I}$ in spherical coordinates is then determined by the usual expression using unit vectors $\hat{e}$:

$$\vec{I}(\mathbf{r},\omega) = \frac{1}{2}\Re[p_\infty^*(v_\theta\hat{e}_\theta + v_\phi\hat{e}_\phi + v_R\hat{e}_R)]. \tag{5}$$

The unknown Fourier coefficients $P_{mn}(a,\omega)$ are determined by integration of the pressure field at $r=a$ over a sphere:

$$P_{mn}(a,\omega) \equiv \iint p_\infty(a,\theta,\phi,\omega) Y_n^m(\theta,\phi)^* d\Omega, \tag{6}$$

with $d\Omega \equiv \sin\theta d\theta d\phi$. The spherical array is designed so that the microphones are located at the quadrature points (θ_j,ϕ_j), $j=1,\cdots,50$, with corresponding integration weights w_j of an efficient algorithm to compute the surface integration in (6). We use an efficient numerical quadrature algorithm derived by Lebedev[5, 6]. This algorithm is invariant with respect to octahedral symmetry, that is, the microphone locations on the spherical cap subtending one of the eight faces of the octahedron are identical (after rotation) on the other seven faces. The 50 element algorithm is important by guaranteeing an exact integration of spherical harmonics when $p_\infty = Y_{n'}^{m'}$ with (6) replaced by the following relation:

$$\sum_{j=1}^{50} w_j Y_{n'}^{m'}(\theta_j,\phi_j) Y_n^m(\theta_j,\phi_j)^* = \delta_{mm'}\delta_{nn'}, \text{ if } n+n' \le 11$$

where δ is the Kronecker delta. The restriction on n in this formula is critical and implies that exact values of P_{mn} are determined (given noiseless pressure data) only when the pressure

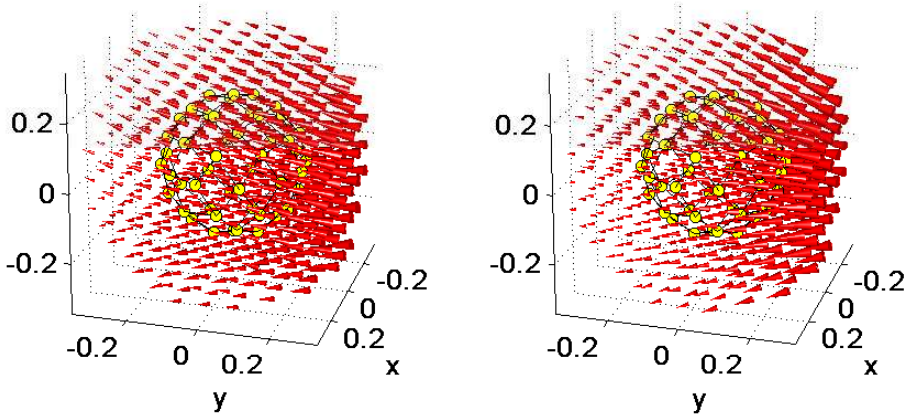

Figure 2: Volumetric intensity Output from the VAIP at 250 Hz and 25dB SNR for a point source at 1.0m is shown on the left versus the exact field shown on the right both plotted on the same scale. The intensity vectors are plotted on a linear scale.

field at $r = a$ is composed of spherical harmonics such that $n \leq 5$. However, even when $n = 6$ most of the orthogonality still remains, so the quadrature algorithm breaks down "gracefully". Given this the quadrature algorithm (6) is approximated by $\hat{P}_{mn}$,

$$\hat{P}_{mn}(a, \omega) = \sum_{j=1}^{50} w_j p_\infty(a, \theta_j, \phi_j, \omega) Y_n^m(\theta_j, \phi_j)^*. \tag{7}$$

where $\hat{P}_{mn} = P_{m'n'}\delta_{mm'}\delta_{nn'}$ when $n+n' \leq 11$. Thus we are guaranteed that $\hat{P}_{mn} = P_{mn}$ as long as $n \leq 5$, so that the first 36 Fourier coefficients are determined without any integration error. For the computation of the pressure and velocity vector in (1) and (4) we choose to use only these accurately computed Fourier coefficients and thus these sums are truncated to $N \leq 5$. We found that there was no gain in accuracy if we used the $n = 6$ approximated Fourier coefficients.

The quadrature weights and locations in cartesian coordinates are easily derived using Lebedev's parameters listed under 11.1 in paper reference [6] and are not reproduced here for brevity.

Simulation Example: Volumetric intensity reconstruction for a point source

An example of the reconstructed intensity fields compared with the exact results for a point source located on the y-axis 1 meter from the origin is shown in fig. 2. Noise was added to the simulated data to give a 25dB signal to noise ratio and the intensity is plotted in the volume $r \leq 0.4$. The cones point to the direction of the intensity vector, and the length (and width) of the cone is proportional to the linear magnitude of the intensity. The center of the base

of the cone is a point in a cubic lattice specifying the locations of the intensity vectors. The lattice spacing in each direction is 0.08 m. The 50 elements (small circles) of the measurement sphere are superimposed in each plot for reference. These results reveal that the direction of the point source (located on axis at y=1.0) is correctly indicated by the reconstructed field (left-hand plots) and the actual location can be found by the intersection of lines collinear with the intensity vectors near the source. Root mean square intensity errors in this case were 7% for $r < 0.2$, 12% for $0.2 < r < 0.3$ and 20% for $0.3 < r < 0.4$. Errors always increase with r since reconstruction of the field outside the array is an ill-posed inverse problem. A very simple regularization filter in n was used to minimize the errors constructed with a brick wall filter using a a series cutoff of $N = 3$ in (1) and (4).

FRONT-END SIGNAL PROCESSING

We summarize the front end theory briefly here and the reader is directed to the references for further information.[9, 10, 11] This theory is used to expand the modes of operation of the VAIP. Although the VAIP can reconstruct intensity fields *without* reference transducers, due to the instantaneous measurement of the pressure data, and identify noise sources by display of the directional intensity vectors radiated from those sources, it is possible to further separate multiple noise sources by using partial field decomposition techniques described in the references. The partial field approach was developed by Hald[9] for NAH and has since found a multitude of industrial applications through the use of the STSF (spatial transformation of sound fields) approach.

Assume M reference transducers recorded simultaneously and Fourier transformed to provide raw spectra represented by $\mathbf{X}(\omega) \equiv (X_1 X_2 \cdots X_M)^t$ (t is transpose) along with the 50 microphone raw spectra $\mathbf{P}(\omega) \equiv (P_1 P_2 \cdots P_{50})^t$ with accompanying noise $\mathbf{N}(\omega) \equiv (N_1 N_2 \cdots N_{50})^t$. The reference transducers are generally attached to candidate (source) machines that are assumed to be random with Gaussian statistics, although they are not necessarily incoherent to one another. A transfer function matrix $\mathbf{H}^{(50\times M)}$ with elements H_{ij} relates the pressure at the i'th microphone and the j'th reference through $\mathbf{P} = \mathbf{HX} + \mathbf{N}$.

The autospectral density $S_{p_i p_i}$ of the i'th microphone is given by an ensemble average E of the raw spectra (using a long time series broken into shorter segments that are each Fourier transformed) of the measured pressure

$$S_{p_i p_i}(\omega) \equiv E[P_i^*(\omega) P_i(\omega)] = \mathbf{H}_i^H \mathbf{S_{xx}} \mathbf{H}_i + S_{n_i n_i}, \tag{8}$$

$$\mathbf{S_{xx}} \equiv E[\mathbf{X}^* \mathbf{X^t}], \tag{9}$$

where $\mathbf{S_{xx}}$ is the $M \times M$ reference cross-spectral density matrix constructed using the ensemble average of the outer products of $\mathbf{X}$, $\mathbf{H}_i$ is the i'th row of $\mathbf{H}$ and the H superscript represents conjugate transpose.

Partial field decomposition techniques all decompose the autospectral density function of a microphone using an inner product of a to-be-determined partial field column vector $\mathbf{\Psi}_i$ of length M, $\mathbf{\Psi}_i = (\Psi_{1i} \Psi_{2i} \cdots \Psi_{Mi})^t$, that is, $S_{p_i p_i} = \mathbf{\Psi}_i^H \mathbf{\Psi}_i + S_{n_i n_i}$. This decomposition

can be accomplished by taking the square root of $\mathbf{S_{xx}} \equiv \sqrt{\mathbf{S_{xx}}}^H \sqrt{\mathbf{S_{xx}}}$, so that (8) becomes

$$S_{p_i p_i}(\omega) = (\sqrt{\mathbf{S_{xx}}}\mathbf{H}_i)^H \sqrt{\mathbf{S_{xx}}}\mathbf{H}_i + S_{n_i n_i}.$$

The partial field components of the i'th microphone are $\mathbf{\Psi}_i \equiv \sqrt{\mathbf{S_{xx}}}\mathbf{H}_i$. A partial field matrix $\mathbf{\Psi}$ is constructed from the $\mathbf{\Psi}_i$ column vectors using $\mathbf{\Psi} = (\mathbf{\Psi}_1 \mathbf{\Psi}_2 \cdots \mathbf{\Psi}_{50})$. The M rows of $\mathbf{\Psi}$ form M partial field holograms, each processed separately for reconstruction of M volumetric intensity fields.

There are two standard procedures for taking the square root of a matrix, the Cholesky decomposition and the singular value decomposition (SVD) and we present results for the first one in this paper. The Cholesky decomosition yields $\mathbf{S_{xx}} = \mathbf{T}^H\mathbf{T}$ where $\mathbf{T}$ is upper triangular and $\sqrt{\mathbf{S_{xx}}} = \mathbf{T}$. It is important to note that in our research we found that the Cholesky method gave identical results to the signal conditioning approach provided in Bendat and Piersol[12] and in [13] A great deal of theory is provided in [12] about the signal conditioning approach which can then be directly applied to understanding results from using the Cholesky decomposition.

The transfer functions $\mathbf{H}_i$ are not of interest here and are eliminated by use of the cross-spectral density column vector $\mathbf{S_{xp}}_i$ defined by

$$\mathbf{S_{xp}}_i \equiv E[\mathbf{X}^*(\omega)P_i(\omega)] = E[\mathbf{X}^*\mathbf{X^t}]\mathbf{H}_i = \mathbf{S_{xx}}\mathbf{H}_i \tag{10}$$

(where $\mathbf{S_{xp}}_i$ is the i'th column of the cross-spectral density matrix $\mathbf{S_{xp}}$) yielding $\mathbf{H}_i = (\mathbf{S_{xx}})^{-1}\mathbf{S_{xp}}_i$. With this elimination we obtain $\mathbf{\Psi}_i = (\mathbf{T}^H)^{-1}\mathbf{S_{xp}}_i$.

An important characteristic of the Cholesky method, and not of the SVD approach, is that the partial fields are dependent upon the order of the columns and rows of $\mathbf{S_{xp}}$.[12] Thus it is necessary to carry out some pre-analysis in the Cholesky approach to set up the order of the references, choosing the most significant reference at a particular frequency to form the first column of $\mathbf{S_{xp}}$. We determine significance by choosing references that have the largest coherence to the microphones, computing the average coherence $\overline{\gamma^2_{x_i p}}$ of the i'th reference to the 50 microphones:

$$\overline{\gamma^2_{x_i p}} \equiv \frac{1}{50}\sum_{j=1}^{50} \gamma^2_{x_i p_j}, \tag{11}$$

where $\gamma^2_{x_i p_j} \equiv |S_{x_i p_j}|^2/(S_{x_i x_i} S_{p_j p_j})$ which allows us to rank the references, $x_m, x_n, \cdots, x_k$, with respect to average coherence for each frequency:

$$\overline{\gamma^2_{x_m p}} > \overline{\gamma^2_{x_n p}} > \cdots > \overline{\gamma^2_{x_k p}}. \tag{12}$$

Here x_m and x_n are the references with the first and second largest average coherence, respectively.

Given this ranking of references we reorder $\mathbf{S_{xx}}$ and $\mathbf{S_{xp}}$ so that the 1st row and column corresponds to the highest rank reference (separate order for each frequency) and so on. The full reconstruction equation becomes, $\mathbf{\Psi} = (\mathbf{T}^H)^{-1}\mathbf{S_{xp}}$. The rows of $\mathbf{\Psi}^{(M\times 50)}$ form M separate holograms ranked in order of importance, each of which can be used to reconstruct the volumetric intensity at a given frequency by replacing $p_\infty(a, \theta_j, \phi_j, \omega)$ in (6) with one of

the rows and computing the intensity vector (5) on a cubic lattice, displaying the results as in fig. 1.

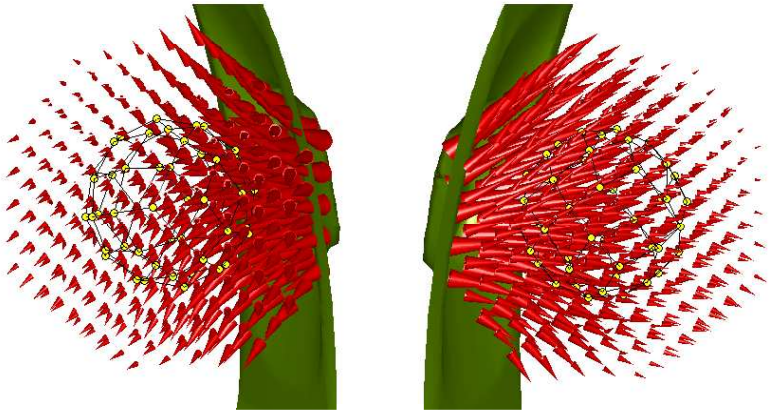

Figure 3: Two views of volumetric intensity results for the 1st partial field with maximum coherence to the window mounted accelerometer. Result indicates that energy is entering the cabin through the window as a result of a window resonance.

In a cooperative effort with NASA Langley and Boeing measurements were made with the 50 element array inside a new Boeing 777 aircraft during test flights for the quiet technology demonstrator program (QTD2).[14] Figure 1 shows the setup and reference accelerometers can also be seen one attached to the window and two on the sidewall directly below. A total of 14 references were used. The VAIP was extremely successful at locating unsuspected noise sources in the aircraft. A typical result is shown in fig. 3 for 240 Hz a frequency at which there was a maximum in the average SPL measured by the array. The pressure and reference data were processed using 200 ensembles each consisting of 2048 points (digitization rate was 12kHz) and the matrices in (9) and (10) were constructed using all the references. Thus 14 partial field holograms were obtained. We found that the only the first two or three partial fields were significant, so that the analysis was not complicated by including so many references. We have plotted the resulting first partial field in the figure corresponding to the window accelerometer (the highest ranking reference in accordance with (12)).

SUMMARY

Many other aspects of operation for the VAIP were not discussed here due to limited space. For example results can be averaged in 1/3 octave bands. Also each ensemble of pressure data

can be processed to produce intensity reconstructions at 1024 frequencies every 0.17 seconds. Inverse transform back to time yields instantaneous intensity vector displays updated every 0.17 s. Self referencing has been used using the microphones at the vertices of the array with great success. We have also used principal component method (SVD) instead of Cholesky and made comparisons between the two approaches. These results will be the subject of future papers and talks. This work was supported by the Office of Naval Research.

References

[1] R. D. Marciniak, "A nearfield, underwater measurement system", J. Acoust. Soc. Am. **66**, 955–964 (1979).

[2] G. Weinreich and E. B. Arnold, "Method for measureing acoustic radiation fields", J. Acoust. Soc. Am. **68**, 404–411 (1980).

[3] M. Park and B. Rafaely, "Sound-field analysis by plane-wave decomposition using spherical microphone array", J. Acoust. Soc. Am. **118**, 3094–3103 (2005).

[4] E. G. Williams, *Fourier Acoustics: Sound Radiation and Nearfield Acoustical Holography* (Academic Press, London, UK) (1999).

[5] V. I. Lebedev, "Values of the nodes and weights of ninth to seventeenth order gauss-markov quatrature formulai invariant under the octahedron group with inversion", Sh. vychisl. Mat. mat. Fiz. **15(1)**, 48–54 (1975).

[6] V. I. Lebedev, "Quadratures on a sphere", USSR Comput. Math. and Math. Phys. **16(2)**, 10–24 (1976).

[7] E. G. Williams, "Regularization methods for near-field acoustical holography", J. Acoust. Soc. Am. **110**, 1976–1988 (2001).

[8] P. C. Hansen, *Rank-Deficient and Discrete Ill-Posed Problems* (Siam, Philadelphia, PA) (1998).

[9] J. Hald, "STSF - a unique technique for scan-based nearfield acoustical holography without restriction on coherence", Technical Report, B&K Technical Review, No. 1 (1989).

[10] H.-S. Kwon and J. S. Bolton, "Partial field decomposition in nearfield acoustical holography by the use of singular value decomposition and partial coherence procedures", in *Proceedings Noise-Con '98*, 649–654 (1998).

[11] K.-U. Nam and Y.-H. Kim, "A partial field decomposition algorithm and its examples for near-field acoustic holography", J. Acoust. Soc. Am. **116**, 172–185 (2004).

[12] J. S. Bendat and A. G. Piersol, *Random Data Analysis and Measurement Procedures*, third edition (John Wiley & Sons, New York, NY) (2000).

[13] M. A. Tomlinson, "Partial source discrimination in near field acoustic holography", Applied Acoustics **57**, 243–261 (1999).

[14] J. Klos and et. al., "Comparison of different measurement technologies of the in-flight assessment of radiated acoustic intensity", in *Proceedings of Noise-Con 2005* (Minneapolis, Minnesota) (2005).